NLO predictions for $t\bar{t}b\bar{b}$ production in association with a light-jet at the LHC

Federico Buccioni

in collaboration with

S. Pozzorini M. Zoller

Universität Zürich[UZH]

FNSNF
Fonds national suisse
Schweizerischer Nationalfonds
Fondo nazionale svizzero
Swiss National Science Foundation

QCD@LCH 2018

TECHNISCHE UNIVERSITÄT DRESDEN

Outline

- $pp \to t\bar{t}H(H \to b\bar{b})$ at the LHC

- Open questions in theory predictions for $t\bar{t} + b$-jets production

- Large NLO K-factor in $pp \to t\bar{t}b\bar{b}$ and scale choices

- NLO QCD predictions for $pp \to t\bar{t}b\bar{b}j$

$pp \to t\bar{t}H(H \to b\bar{b})$ at the LHC

The determination of the Higgs boson coupling to the top quark is a crucial test of the SM

top quark Yukawa coupling can be determined through measurements of

$t\bar{t}H$ **associated production**

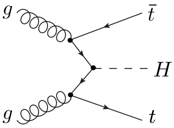

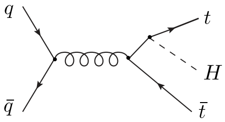

$pp \to t\bar{t}H(H \to b\bar{b})$ at the LHC

The determination of the Higgs boson coupling to the top quark is a crucial test of the SM

top quark Yukawa coupling can be determined through measurements of

$t\bar{t}H$ **associated production**

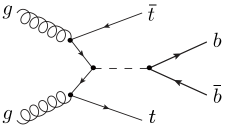

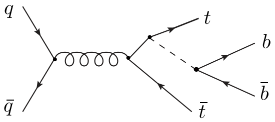

H branching ratio is dominated by $H \to b\bar{b}$ decay: channel with highest statistics

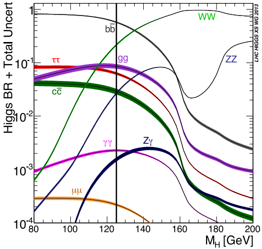

$pp \to t\bar{t}H(H \to b\bar{b})$ at the LHC

The determination of the Higgs boson coupling to the top quark is a crucial test of the SM

top quark Yukawa coupling can be determined through measurements of

$t\bar{t}H$ **associated production**

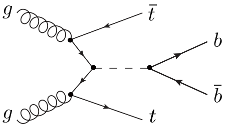

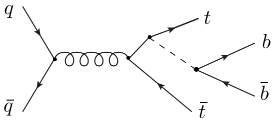

H branching ratio is dominated by $H \to b\bar{b}$ decay: channel with highest statistics

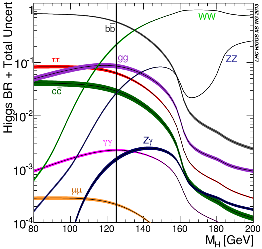

But: this channel suffers from a large, irreducible QCD background

$pp \to t\bar{t}+$ b-jets production

signal

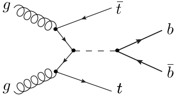

background

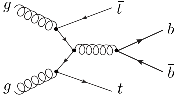

An accurate understanding and description of the background is mandatory for the sensitivity of $t\bar{t}H(H \to b\bar{b})$ analyses

$t\bar{t}H$ discovery at the LHC

⇒ focus on **Higgs couplings**

$t\bar{t}H$ discovery at the LHC

EUROPEAN ORGANISATION FOR NUCLEAR RESEARCH (CERN)

Submitted to: PLB

CERN-EP-2018-138
4th June 2018

Observation of Higgs boson production in association with a top quark pair at the LHC with the ATLAS detector

6.3 std. dev. ←

5.2 std. dev. →

PHYSICAL REVIEW LETTERS **120**, 231801 (2018)

Editors' Suggestion | Featured in Physics

Observation of $t\bar{t}H$ Production

A. M. Sirunyan *et al.**
(CMS Collaboration)

(Received 8 April 2018; revised manuscript received 1 May 2018; published 4 June 2018)

$t\bar{t}H$ discovery at the LHC

$\Rightarrow$ focus on **Higgs couplings**

$t\bar{t}H$ discovery at the LHC

EUROPEAN ORGANISATION FOR NUCLEAR RESEARCH (CERN)

Submitted to: PLB

CERN-EP-2018-138
4th June 2018

Observation of Higgs boson production in association with a top quark pair at the LHC with the ATLAS detector

6.3 std. dev.

5.2 std. dev.

PHYSICAL REVIEW LETTERS **120**, 231801 (2018)

Editors' Suggestion | Featured in Physics

Observation of $t\bar{t}H$ Production

A. M. Sirunyan *et al.*
(CMS Collaboration)

(Received 8 April 2018; revised manuscript received 1 May 2018; published 4 June 2018)

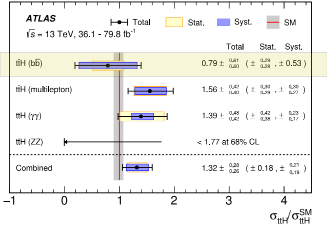

dominated by systematics

Uncertainty source	$\Delta\sigma_{t\bar{t}H}/\sigma_{t\bar{t}H}$ [%]
Theory uncertainties (modelling)	11.9
$t\bar{t}$ + heavy flavour	9.9
$t\bar{t}H$	6.0
Non-$t\bar{t}H$ Higgs boson production modes	1.5
Other background processes	2.2
Experimental uncertainties	9.3
Fake leptons	5.2
Jets, E_T^{miss}	4.9
Electrons, photons	3.2
Luminosity	3.0
τ-lepton	2.5
Flavour tagging	1.8
MC statistical uncertainties	4.4

uncertainty dominated by
$t\bar{t}$ + heavy flavour modelling in the $H \to b\bar{b}$ analyses

State of the art for $t\bar{t}b\bar{b}$ predictions

- First fixed order NLO QCD predictions for $pp \to t\bar{t}b\bar{b}$ [Bredenstein et al. '09, Bevilacqua et al. '09]
  first estimate of theory uncertainties + first NLO calculation for $2 \to 4$

- First NLOPS simulation for $t\bar{t}b\bar{b}$ production in `Powhel` [Garzelli et al. '13]
  ME in the 5F scheme $(m_b = 0)$ + Powheg matching for the parton shower
  since recently available also in the 4F scheme [Bevilacqua et al. '17]

- NLOPS generator for $t\bar{t}b\bar{b}$ with massive b-quark in `OpenLoops+Sherpa` [Cascioli et al. '14]
  `OpenLoops` for 1-loop automation + `Sherpa` employing MC@NLO matching

- NLOPS generator for $t\bar{t}$ + b-jet production in 4F scheme in `OpenLoops+Powheg` [Ježo et al. '18]
  `OpenLoops` for amplitudes automation + Powheg matching in `Powheg-Box-Res`

  thorough investigation of uncertainties related to matching method and parton shower modelling

- $t\bar{t}$ + b-jets simulations in the 4F scheme also available in
  `MG5_aMC@NLO` [Alwall et al. '14] and `Matchbox` [Plaetzer, Reuschle et al.]

$t\bar{t} + b$-jets production in the 4F scheme

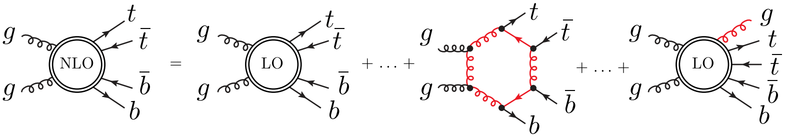

In the **4F scheme**: ***b*-quarks** are treated as **massive**

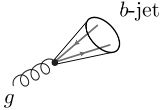

⇒ calculation of the ME can be extended to the entire the phase space

⇒ no singularities in $g \to b\bar{b}$ splittings. Safe collinear regime with $g \to b$-jet

On the other hand:

× non-trivial multi-scale multi-particle QCD process

× large scales separation between $t\bar{t}$ and $b\bar{b}$ systems

$m_b \sim 5$ GeV $t\bar{t}$ typical scale up to ~ 500 GeV

scale choice and estimation of theoretical uncertainties non trivial

$t\bar{t}$ + b-jets production in the 4F scheme

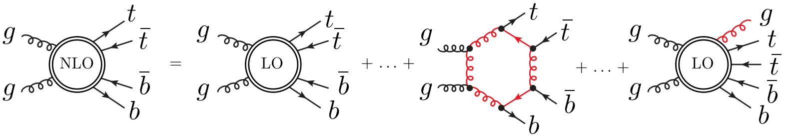

In the **4F scheme**: ***b*-quarks** are treated as **massive**

⇒ calculation of the ME can be extended to the entire the phase space

⇒ no singularities in $g \to b\bar{b}$ splittings. Safe collinear regime with $g \to b$-jet

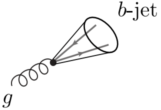

On the other hand:

× non-trivial multi-scale multi-particle QCD process

× large scales separation between $t\bar{t}$ and $b\bar{b}$ systems

$m_b \sim 5$ GeV $\quad$ $t\bar{t}$ typical scale up to ~ 500 GeV

scale choice and estimation of theoretical uncertainties non trivial

XS dominated by FS $g \to b\bar{b}$ splittings

[Ježo et al. '18]

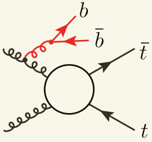

it supports using $m_b > 0$

Discrepancies in $t\bar{t}b\bar{b}$ NLOPS generators

Standard factor-2 μ_R variations $\sim 30\%$ NLO scale dependence

But: discrepancies between different NLOPS generators significantly exceed NLO scale variations

Most sensitive distribution: light-jet p_T spectrum
up to 100% shape differences in the 100-200 GeV region

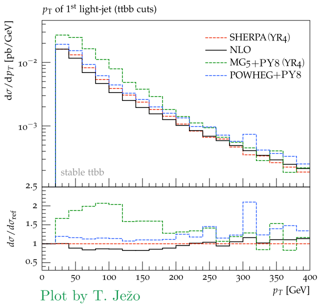

Plot by T. Ježo

Discrepancies in $t\bar{t}b\bar{b}$ NLOPS generators

Standard factor-2 μ_R variations $\sim 30\%$ NLO scale dependence

But: discrepancies between different NLOPS generators significantly exceed NLO scale variations

Most sensitive distribution: light-jet p_T spectrum
up to 100% shape differences in the 100-200 GeV region

Most likely **hypothesis** on origin of NLOPS differences:
interplay between PS and **large NLO $t\bar{t}b\bar{b}$ K-factor**
which enters the PS matching in the soft regime

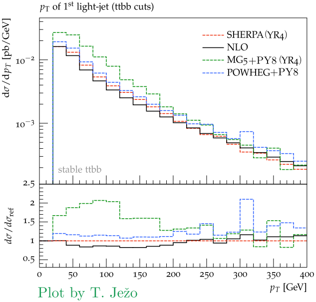

Plot by T. Ježo

Discrepancies in $t\bar{t}b\bar{b}$ NLOPS generators

Standard factor-2 μ_R variations $\sim 30\%$ NLO scale dependence

But: discrepancies between different NLOPS generators significantly exceed NLO scale variations

Most sensitive distribution: light-jet p_T spectrum
up to 100% shape differences in the 100-200 GeV region

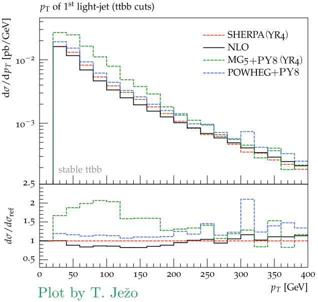

Plot by T. Ježo

Most likely **hypothesis** on origin of NLOPS differences:
interplay between PS and **large NLO $t\bar{t}b\bar{b}$ K-factor** which enters the PS matching in the soft regime

(1) origin of large K-factor to be understood

Discrepancies in $t\bar{t}b\bar{b}$ NLOPS generators

Standard factor-2 μ_R variations $\sim 30\%$ NLO scale dependence

But: discrepancies between different NLOPS generators significantly exceed NLO scale variations

Most sensitive distribution: light-jet p_T spectrum
up to 100% shape differences in the 100-200 GeV region

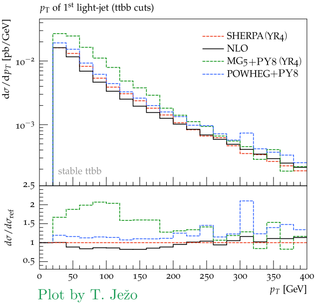

Plot by T. Ježo

Most likely **hypothesis** on origin of NLOPS differences:
interplay between PS and **large NLO $t\bar{t}b\bar{b}$ K-factor**
which enters the PS matching in the soft regime

(1) origin of large K-factor to be understood

(2) **Idea**: reduce uncertainties discarding less accurate NLOPS predictions
by means of a benchmark $p_{T,j}$ spectrum with uncertainty well below 100%
Motivation for $pp \to t\bar{t}b\bar{b}j$ at NLO QCD

Discrepancies in $t\bar{t}b\bar{b}$ NLOPS generators

Standard factor-2 μ_R variations $\sim 30\%$ NLO scale dependence

But: discrepancies between different NLOPS generators significantly exceed NLO scale variations

Most sensitive distribution: light-jet p_T spectrum
up to 100% shape differences in the 100-200 GeV region

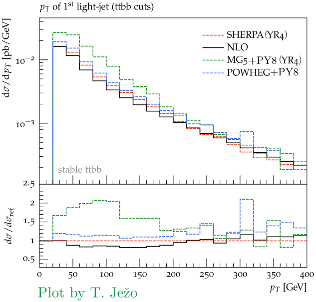

Plot by T. Ježo

Most likely **hypothesis** on origin of NLOPS differences:
interplay between PS and **large NLO $t\bar{t}b\bar{b}$ K-factor**
which enters the PS matching in the soft regime

(1) origin of large K-factor to be understood

(2) **Idea**: reduce uncertainties discarding less accurate NLOPS predictions by means of a benchmark $p_{T,j}$ spectrum with uncertainty well below 100%
Motivation for $pp \to t\bar{t}b\bar{b}j$ at NLO QCD

This talk

Large $t\bar{t}b\bar{b}$ NLO K-factor

Input parameters, PDFs and scale choices [Ježo et al. '18]

$$m_b = 4.75 \text{ GeV} \qquad m_t = 172.5 \text{ GeV}$$

dynamic scales

$$\mu_R = \sqrt{\mu_{t\bar{t}}\mu_{b\bar{b}}} \quad \text{with} \quad \mu_{b\bar{b}} = \sqrt{E_{T,b}E_{T,\bar{b}}} \quad \mu_{t\bar{t}} = \sqrt{E_{T,t}E_{T,\bar{t}}}$$

$$\mu_F = \frac{H_\mathrm{T}}{2} = \frac{1}{2} \sum_{i=t,\bar{t},b,\bar{b},j} E_{T,i}$$

NLO PDFs are used throughout: both at LO and NLO

`NNPDF_nlo_as_0118_nf_4` with $\alpha_s^{4\mathrm{f}}$

Large $t\bar{t}b\bar{b}$ NLO K-factor

Input parameters, PDFs and scale choices [Ježo et al. '18]

$$m_b = 4.75 \text{ GeV} \qquad m_t = 172.5 \text{ GeV}$$

dynamic scales

$$\mu_R = \sqrt{\mu_{t\bar{t}}\mu_{b\bar{b}}} \quad \text{with} \quad \mu_{b\bar{b}} = \sqrt{E_{T,b}E_{T,\bar{b}}} \quad \mu_{t\bar{t}} = \sqrt{E_{T,t}E_{T,\bar{t}}}$$

$$\mu_F = \frac{H_T}{2} = \frac{1}{2}\sum_{i=t,\bar{t},b,\bar{b},j} E_{T,i}$$

NLO PDFs are used throughout: both at LO and NLO

NNPDF_nlo_as_0118_nf_4 with α_s^{4f}

The NLO QCD cross sections for $pp \to t\bar{t}b\bar{b}$ feature a large K-factor

K-factor

$N_{b-jets\geq 0}$: 2.06

$N_{b-jets\geq 1}$: 1.92

$N_{b-jets\geq 2}$: 1.79

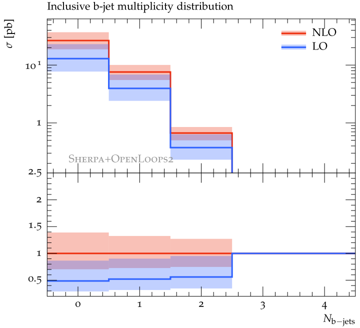

Large $t\bar{t}b\bar{b}$ NLO K-factor

Input parameters, PDFs and scale choices [Ježo et al. '18]

$$m_b = 4.75 \text{ GeV} \qquad m_t = 172.5 \text{ GeV}$$

$$\mu_R = \sqrt{\mu_{t\bar{t}}\mu_{b\bar{b}}} \quad \text{with} \quad \mu_{b\bar{b}} = \sqrt{E_{T,b}E_{T,\bar{b}}} \quad \mu_{t\bar{t}} = \sqrt{E_{T,t}E_{T,\bar{t}}}$$

dynamic scales

$$\mu_F = \frac{H_{\mathrm{T}}}{2} = \frac{1}{2} \sum_{i=t,\bar{t},b,\bar{b},j} E_{T,i}$$

NLO PDFs are used throughout: both at LO and NLO

`NNPDF_nlo_as_0118_nf_4` with $\alpha_s^{4\mathrm{f}}$

The NLO QCD cross sections for $pp \to t\bar{t}b\bar{b}$ feature a large K-factor

more realistic picture of perturbative convergence but much bigger K-factor wrt using LO α_S + PDFs for σ_{LO}

K-factor

$N_{b-jets\geq 0}$: 2.06

$N_{b-jets\geq 1}$: 1.92

$N_{b-jets\geq 2}$: 1.79

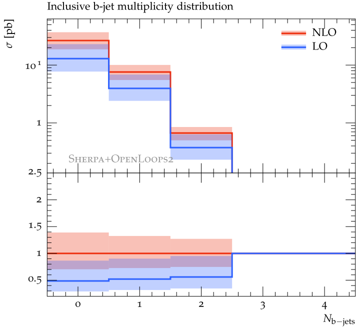

Large $t\bar{t}b\bar{b}$ NLO K-factor

The K-factor is large and stable for cross sections and distributions

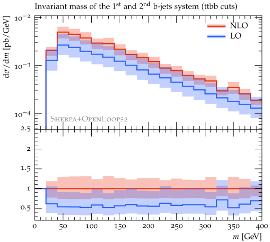

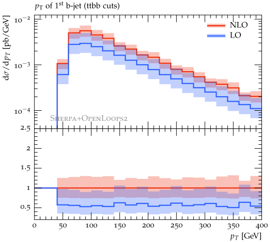

Such a large K-factor poses a question:

are corrections beyond NLO larger than factor 2 scale variations?

↓

origin of large K-factor needs to be understood

Large $t\bar{t}b\bar{b}$ NLO K-factor

The K-factor is large and stable for cross sections and distributions

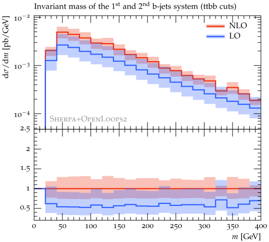

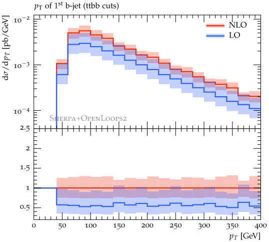

Such a large K-factor poses a question:

are corrections beyond NLO larger than factor 2 scale variations?

origin of large K-factor needs to be understood

Hypotheses on origin of large K-factor:

Large $t\bar{t}b\bar{b}$ NLO K-factor

The K-factor is large and stable for cross sections and distributions

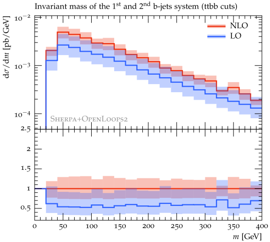

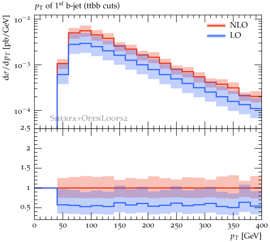

Such a large K-factor poses a question:

are corrections beyond NLO larger than factor 2 scale variations?

↓

origin of large K-factor needs to be understood

Hypotheses on origin of large K-factor:

(a) sizeable NLO real emission contribution:

σ_{NLO} strongly enhanced by hard jet radiation interpreted as $t\bar{t}gg(g \to b\bar{b})$

interplay with large mass gap in $t\bar{t}$ and $b\bar{b}$ systems $(m_b, p_{T,b} \ll m_t) \Rightarrow p_{T,b} < p_{T,j} < m_t$

Large $t\bar{t}b\bar{b}$ NLO K-factor

The K-factor is large and stable for cross sections and distributions

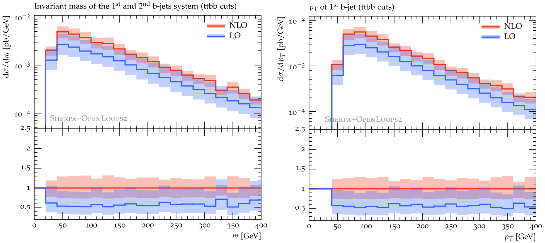

Such a large K-factor poses a question:
are corrections beyond NLO larger than factor 2 scale variations?

origin of large K-factor needs to be understood

Hypotheses on origin of large K-factor:

(a) sizeable NLO real emission contribution:

σ_{NLO} strongly enhanced by hard jet radiation interpreted as $t\bar{t}gg(g \to b\bar{b})$

interplay with large mass gap in $t\bar{t}$ and $b\bar{b}$ systems $(m_b, p_{T,b} \ll m_t) \Rightarrow p_{T,b} < p_{T,j} < m_t$

it enters as a “new process” described at LO ⇒ potentially large NLO QCD corrections

Large $t\bar{t}b\bar{b}$ NLO K-factor

The K-factor is large and stable for cross sections and distributions

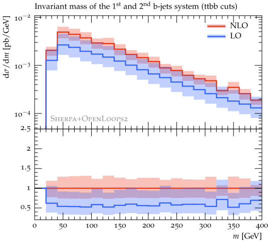

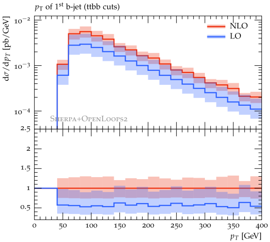

Such a large K-factor poses a question:

are corrections beyond NLO larger than factor 2 scale variations?

↓

origin of large K-factor needs to be understood

Hypotheses on origin of large K-factor:

(a) sizeable NLO real emission contribution:

σ_{NLO} strongly enhanced by hard jet radiation interpreted as $t\bar{t}gg(g \to b\bar{b})$

interplay with large mass gap in $t\bar{t}$ and $b\bar{b}$ systems $(m_b, p_{T,b} \ll m_t) \Rightarrow p_{T,b} < p_{T,j} < m_t$

it enters as a "new process" described at LO ⇒ potentially large NLO QCD corrections

(b) non-optimal μ_R scale choice:

an improved μ_R choice might reduce the K-factor and also mitigate the NLOPS discrepancies

(a) Mass effects on $pp \to t\bar{t}b\bar{b}$ X sections

Aim: try to understand if the large K-factor is related to $m_t \gg m_b$

Idea: study the NLO K-factor for different mass configurations by means of $m^* = \sqrt{m_b m_t}$
$m^* \sim 28.62$ GeV

(a) Mass effects on $pp \to t\bar{t}b\bar{b}$ X sections

Aim: try to understand if the large K-factor is related to $m_t \gg m_b$

Idea: study the NLO K-factor for different mass configurations by means of $m^* = \sqrt{m_b m_t}$
$m^* \sim 28.62$ GeV

masses [GeV]		$\sigma_{N_{b\text{-jets}\geq 0}}$ [pb]			$\sigma_{N_{b\text{-jets}\geq 1}}$ [pb]			$\sigma_{N_{b\text{-jets}\geq 2}}$ [pb]		
m_b	m_t	LO	NLO	$\frac{\text{NLO}}{\text{LO}}$	LO	NLO	$\frac{\text{NLO}}{\text{LO}}$	LO	NLO	$\frac{\text{NLO}}{\text{LO}}$
4.75	172.5	12.94	26.61	2.06	3.955	7.593	1.92	0.374	0.669	1.79
28.62	28.62	321.1	642.4	2.0	165.3	317.7	1.92	34.61	63.42	1.83
28.62	172.5	0.999	1.911	1.9	0.752	1.400	1.86	0.245	0.437	1.78
172.5	172.5	0.013	0.023	1.82	0.013	0.023	1.81	$9.31 \cdot 10^{-3}$	$1.67 \cdot 10^{-2}$	1.79

Dynamic scales choice:

$$\mu_R = \prod_{i=t,\bar{t},b,\bar{b}} E_{T,i}^{1/4}$$

$$\mu_F = \frac{H_T}{2}$$

(a) Mass effects on $pp \to t\bar{t}b\bar{b}$ X sections

Aim: try to understand if the large K-factor is related to $m_t \gg m_b$

Idea: study the NLO K-factor for different mass configurations by means of $m^* = \sqrt{m_b m_t}$
$m^* \sim 28.62$ GeV

masses [GeV]		$\sigma_{N_{b\text{-jets}\geq 0}}$ [pb]			$\sigma_{N_{b\text{-jets}\geq 1}}$ [pb]			$\sigma_{N_{b\text{-jets}\geq 2}}$ [pb]		
m_b	m_t	LO	NLO	$\frac{\text{NLO}}{\text{LO}}$	LO	NLO	$\frac{\text{NLO}}{\text{LO}}$	LO	NLO	$\frac{\text{NLO}}{\text{LO}}$
4.75	172.5	12.94	26.61	2.06	3.955	7.593	1.92	0.374	0.669	1.79
28.62	28.62	321.1	642.4	2.0	165.3	317.7	1.92	34.61	63.42	1.83
28.62	172.5	0.999	1.911	1.9	0.752	1.400	1.86	0.245	0.437	1.78
172.5	172.5	0.013	0.023	1.82	0.013	0.023	1.81	$9.31 \cdot 10^{-3}$	$1.67 \cdot 10^{-2}$	1.79

Dynamic scales choice:

$$\mu_R = \prod_{i=t,\bar{t},b,\bar{b}} E_{T,i}^{1/4}$$

$$\mu_F = \frac{H_T}{2}$$

× Large K-factor stable
wrt variations of m_t, m_b gap

(a) Mass effects on $pp \to t\bar{t}b\bar{b}$ X sections

Aim: try to understand if the large K-factor is related to $m_t \gg m_b$

Idea: study the NLO K-factor for different mass configurations by means of $m^* = \sqrt{m_b m_t}$
$m^* \sim 28.62$ GeV

masses [GeV]		$\sigma_{N_{b\text{-jets}\geq 0}}$ [pb]			$\sigma_{N_{b\text{-jets}\geq 1}}$ [pb]			$\sigma_{N_{b\text{-jets}\geq 2}}$ [pb]		
m_b	m_t	LO	NLO	$\frac{\text{NLO}}{\text{LO}}$	LO	NLO	$\frac{\text{NLO}}{\text{LO}}$	LO	NLO	$\frac{\text{NLO}}{\text{LO}}$
4.75	172.5	12.94	26.61	2.06	3.955	7.593	1.92	0.374	0.669	1.79
28.62	28.62	321.1	642.4	2.0	165.3	317.7	1.92	34.61	63.42	1.83
28.62	172.5	0.999	1.911	1.9	0.752	1.400	1.86	0.245	0.437	1.78
172.5	172.5	0.013	0.023	1.82	0.013	0.023	1.81	$9.31 \cdot 10^{-3}$	$1.67 \cdot 10^{-2}$	1.79

Dynamic scales choice:

$$\mu_R = \prod_{i=t,\bar{t},b,\bar{b}} E_{T,i}^{1/4}$$

$$\mu_F = \frac{H_T}{2}$$

× Large K-factor stable wrt variations of m_t, m_b gap

✓ good shapes in distributions

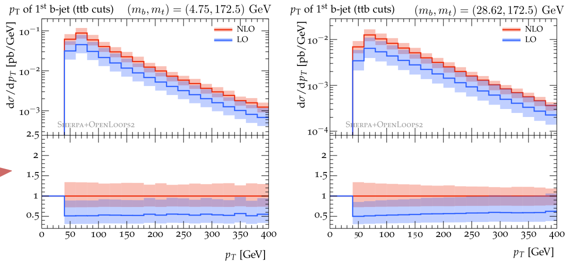

(a) Mass effects on $pp \to t\bar{t}b\bar{b}$ X sections

Aim: try to understand if the large K-factor is related to $m_t \gg m_b$

Idea: study the NLO K-factor for different mass configurations by means of $m^* = \sqrt{m_b m_t}$
$m^* \sim 28.62$ GeV

masses [GeV]		$\sigma_{N_{b\text{-jets}\geq 0}}$ [pb]			$\sigma_{N_{b\text{-jets}\geq 1}}$ [pb]			$\sigma_{N_{b\text{-jets}\geq 2}}$ [pb]		
m_b	m_t	LO	NLO	$\frac{\text{NLO}}{\text{LO}}$	LO	NLO	$\frac{\text{NLO}}{\text{LO}}$	LO	NLO	$\frac{\text{NLO}}{\text{LO}}$
4.75	172.5	12.94	26.61	2.06	3.955	7.593	1.92	0.374	0.669	1.79
28.62	28.62	321.1	642.4	2.0	165.3	317.7	1.92	34.61	63.42	1.83
28.62	172.5	0.999	1.911	1.9	0.752	1.400	1.86	0.245	0.437	1.78
172.5	172.5	0.013	0.023	1.82	0.013	0.023	1.81	$9.31 \cdot 10^{-3}$	$1.67 \cdot 10^{-2}$	1.79

Dynamic scales choice:

$$\mu_R = \prod_{i=t,\bar{t},b,\bar{b}} E_{T,i}^{1/4}$$

$$\mu_F = \frac{H_T}{2}$$

× Large K-factor stable wrt variations of m_t, m_b gap

✓ good shapes in distributions

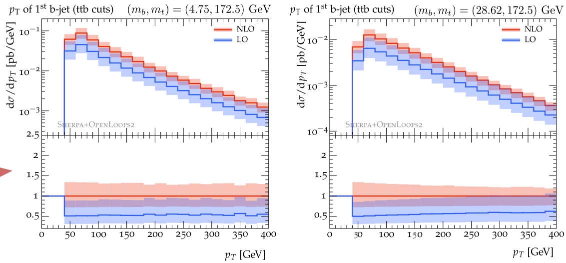

⇒ **hypothesis (a) disfavoured**

(b) Renormalisation scale choice

If no mass gap i.e. $m_b = m_t$ there would be a natural choice $\Rightarrow \mu_R = m_t$

A direct generalisation could be $\mu_R = \sqrt{m_b m_t}$

(b) Renormalisation scale choice

If no mass gap i.e. $m_b = m_t$ there would be a natural choice $\Rightarrow \mu_R = m_t$

A direct generalisation could be $\mu_R = \sqrt{m_b m_t}$ → moderate K-factor for different m_b, m_t

Physical case: $m_b = 4.75$ GeV, $m_t = 172.5$ GeV

$\sqrt{m_b m_t} \sim 28.62$ GeV → fixed μ_R scale

✓ reduced K-factor ~ 1.47

× enhanced shape distortion in distributions

× unreliable scale uncertainties

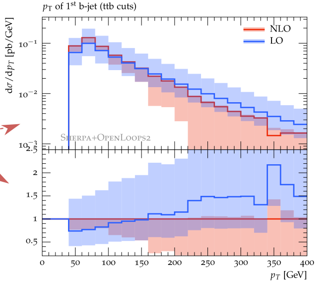

(b) Renormalisation scale choice

If no mass gap i.e. $m_b = m_t$ there would be a natural choice $\Rightarrow \mu_R = m_t$

A direct generalisation could be $\mu_R = \sqrt{m_b m_t}$ ⟶ moderate K-factor for different m_b, m_t

Physical case: $m_b = 4.75$ GeV, $m_t = 172.5$ GeV

$\sqrt{m_b m_t} \sim 28.62$ GeV $\rightarrow$ fixed μ_R scale

✓ reduced K-factor ~ 1.47

× enhanced shape distortion in distributions

× unreliable scale uncertainties

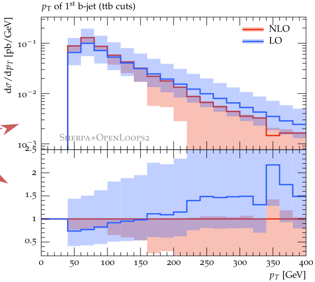

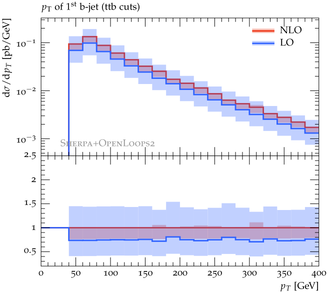

motivates a reduced dynamic $\mu_R = \xi \prod_{i=t,\bar{t},b,\bar{b}} E_{T,i}^{1/4}$

Example: $\xi = 1/3$

✓ reduced K-factor

✓ no shape distortions in distributions

✓ $\sim 20\%$ scale uncertainties

(b) Renormalisation scale dependence

Both at LO and NLO scale uncertainties are dominated by μ_R variations.

Default choice of scale: $\mu_R = \mu_{def} \equiv \prod_{i=t,\bar{t},b,\bar{b}} E_{T,i}^{1/4}$

Average value $\bar{\mu}_{def} \Rightarrow$ $N_{b\geq 0} \sim 73$ GeV $N_{b\geq 1} \sim 93$ GeV $N_{b\geq 2} \sim 124$ GeV

(b) Renormalisation scale dependence

Both at LO and NLO scale uncertainties are dominated by μ_R variations.

Default choice of scale: $\mu_R = \mu_{def} \equiv \prod_{i=t,\bar{t},b,\bar{b}} E_{T,i}^{1/4}$

Average value $\bar{\mu}_{def} \Rightarrow \quad N_{b\geq 0} \sim 73$ GeV $\quad N_{b\geq 1} \sim 93$ GeV $\quad N_{b\geq 2} \sim 124$ GeV

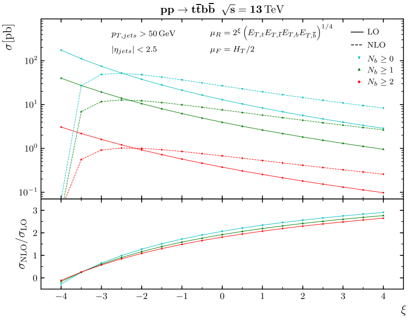

$\mu_R = 2^\xi \left(E_{T,t}E_{T,\bar{t}}E_{T,b}E_{T,\bar{b}}\right)^{1/4}$

(b) Renormalisation scale dependence

Both at LO and NLO scale uncertainties are dominated by μ_R variations.

Default choice of scale: $\mu_R = \mu_{def} \equiv \prod_{i=t,\bar{t},b,\bar{b}} E_{T,i}^{1/4}$

Average value $\bar{\mu}_{def} \Rightarrow$ $N_{b\geq 0} \sim 73$ GeV $N_{b\geq 1} \sim 93$ GeV $N_{b\geq 2} \sim 124$ GeV

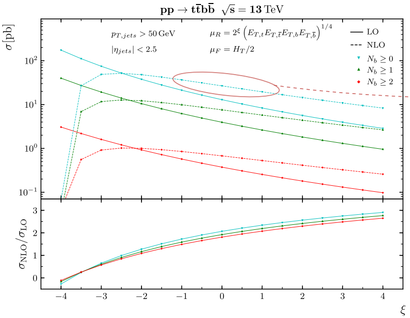

$\mu_R = 2^\xi \left(E_{T,t}E_{T,\bar{t}}E_{T,b}E_{T,\bar{b}}\right)^{1/4}$

factor 2 variation: ∼ 27% NLO uncertainty

(b) Renormalisation scale dependence

Both at LO and NLO scale uncertainties are dominated by μ_R variations.

Default choice of scale: $\mu_R = \mu_{def} \equiv \prod_{i=t,\bar{t},b,\bar{b}} E_{T,i}^{1/4}$

Average value $\bar{\mu}_{def} \Rightarrow$ $N_{b\geq 0} \sim 73$ GeV $N_{b\geq 1} \sim 93$ GeV $N_{b\geq 2} \sim 124$ GeV

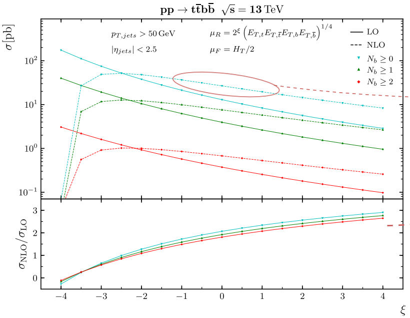

$\mu_R = 2^\xi \left(E_{T,t}E_{T,\bar{t}}E_{T,b}E_{T,\bar{b}}\right)^{1/4}$

factor 2 variation: $\sim 27\%$ NLO uncertainty

similar K-factor for different b-jets multiplicities

(b) Renormalisation scale dependence

Both at LO and NLO scale uncertainties are dominated by μ_R variations.

Default choice of scale: $\mu_R = \mu_{def} \equiv \prod_{i=t,\bar{t},b,\bar{b}} E_{T,i}^{1/4}$

Average value $\bar{\mu}_{def} \Rightarrow$ $N_{b\geq 0} \sim 73$ GeV $N_{b\geq 1} \sim 93$ GeV $N_{b\geq 2} \sim 124$ GeV

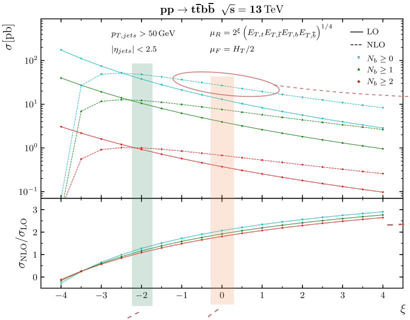

$\mu_R = 2^{\xi}\left(E_{T,t}E_{T,\bar{t}}E_{T,b}E_{T,\bar{b}}\right)^{1/4}$

factor 2 variation: $\sim 27\%$ NLO uncertainty

similar K-factor for different b-jets multiplicities

default

region where K-factor ~ 1, close the maximum of the NLO XS

(b) Renormalisation scale dependence

Both at LO and NLO scale uncertainties are dominated by μ_R variations.

Default choice of scale: $\mu_R = \mu_{def} \equiv \prod_{i=t,\bar{t},b,\bar{b}} E_{T,i}^{1/4}$

Average value $\bar{\mu}_{def} \Rightarrow$ $N_{b\geq 0} \sim 73$ GeV $N_{b\geq 1} \sim 93$ GeV $N_{b\geq 2} \sim 124$ GeV

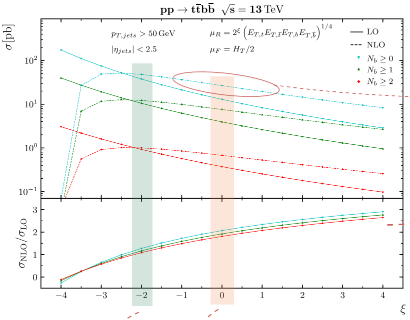

$\mu_R = 2^{\xi}\left(E_{T,t}E_{T,\bar{t}}E_{T,b}E_{T,\bar{b}}\right)^{1/4}$

factor 2 variation: $\sim 27\%$ NLO uncertainty

similar K-factor for different b-jets multiplicities

a factor 2-4 reduction of μ_R brings K**-factor close to 1** and scale uncertainty $\sim 20\%$

default

region where K-factor ~ 1, close the maximum of the NLO XS

(b) Renormalisation scale dependence

Both at LO and NLO scale uncertainties are dominated by μ_R variations.

Default choice of scale: $\mu_R = \mu_{def} \equiv \prod_{i=t,\bar{t},b,\bar{b}} E_{T,i}^{1/4}$

Average value $\bar{\mu}_{def} \Rightarrow$ $N_{b\geq 0} \sim 73$ GeV $N_{b\geq 1} \sim 93$ GeV $N_{b\geq 2} \sim 124$ GeV

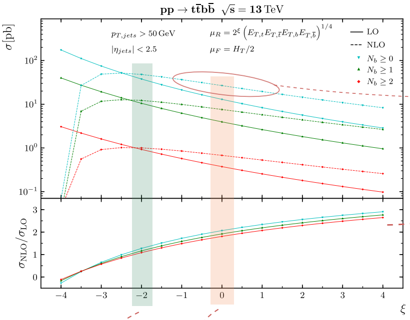

$\mu_R = 2^\xi \left(E_{T,t}E_{T,\bar{t}}E_{T,b}E_{T,\bar{b}}\right)^{1/4}$

factor 2 variation: $\sim 27\%$ NLO uncertainty

similar K-factor for different b-jets multiplicities

a factor 2-4 reduction of μ_R brings **K-factor close to 1** and scale uncertainty $\sim 20\%$

default

region where K-factor ~ 1, close the maximum of the NLO XS

it supports hypothesis (b)

(b) Alternative dynamic μ_R choice

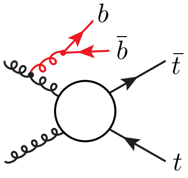

Alternative μ_R based on k_T of splittings in dominant $t\bar{t}b\bar{b}$ topologies

$$\mu_R = \mu_{gbb} \equiv \left(E_{T,t} E_{T,\bar{t}} E_{T,b\bar{b}}\, m_{b\bar{b}}\right)^{1/4}$$

In general it is a harder scale than μ_{def}: $\bar{\mu}_{gbb} \sim 125$ GeV $\bar{\mu}_{def} \sim 93$ GeV

→ hence a larger K-factor than μ_{def} at central value

(b) Alternative dynamic μ_R choice

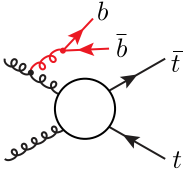

Alternative μ_R based on k_T of splittings in dominant $t\bar{t}b\bar{b}$ topologies

$$\mu_R = \mu_{gbb} \equiv \left(E_{T,t} E_{T,\bar{t}} E_{T,b\bar{b}}\, m_{b\bar{b}}\right)^{1/4}$$

In general it is a harder scale than μ_{def}: $\bar{\mu}_{gbb} \sim 125$ GeV $\bar{\mu}_{def} \sim 93$ GeV

→ hence a larger K-factor than μ_{def} at central value

Example: $\frac{\mu_{gbb}}{4} \Rightarrow K$-factor ~ 1.4 yields 20-25% scale uncertainty at NLO

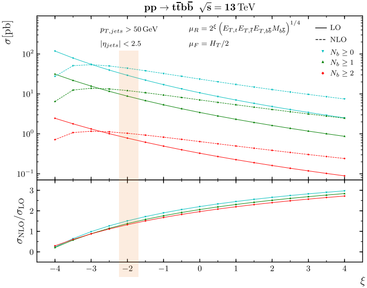

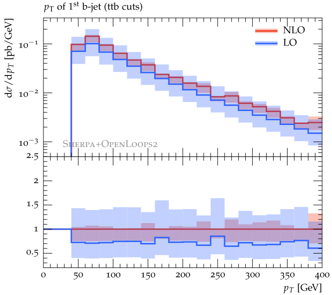

✓ good shape of K-factor for relevant distributions

$pp \to t\bar{t}b\bar{b}j$ at NLO QCD

First jet emission from matrix element $\Rightarrow$ accurate benchmark for p_T of light jet radiation

Idea: look at $p_{T,j}$ spectrum in $t\bar{t}b\bar{b}$ using reduced μ_R scales and validate against NLO prediction

$pp \to t\bar{t}b\bar{b}j$ at NLO QCD

First jet emission from matrix element $\Rightarrow$ accurate benchmark for p_T of light jet radiation

Idea: look at $p_{T,j}$ spectrum in $t\bar{t}b\bar{b}$ using reduced μ_R scales and validate against NLO prediction

We consider $pp \to t\bar{t}b\bar{b}j$ at 13 TeV centre of mass energy

- top quark stable, not decayed
- jets reconstructed using anti-k_T algorithm
  as implemented in `FastJet-3.2`
- $\Delta R = 0.4, \quad p_T > 50$ GeV, $\quad |\eta| < 2.5$
- input parameters and scales choices as in $t\bar{t}b\bar{b}$

$pp \to t\bar{t}b\bar{b}j$ at NLO QCD

First jet emission from matrix element $\Rightarrow$ accurate benchmark for p_T of light jet radiation

Idea: look at $p_{T,j}$ spectrum in $t\bar{t}b\bar{b}$ using reduced μ_R scales and validate against NLO prediction

We consider $pp \to t\bar{t}b\bar{b}j$ at 13 TeV centre of mass energy

- top quark stable, not decayed
- jets reconstructed using anti-k_T algorithm as implemented in `FastJet-3.2`
- $\Delta R = 0.4, \quad p_T > 50$ GeV, $\quad |\eta| < 2.5$
- input parameters and scales choices as in $t\bar{t}b\bar{b}$

this talk

b-jets tagging

"single-tagged": b or $\bar{b}$ quark content

"double-tagged": $b\bar{b}$ content

generic b-jet: b, $\bar{b}$ and $b\bar{b}$ equally counted

important for comparisons against PS

$pp \to t\bar{t}b\bar{b}j$ at NLO QCD

First jet emission from matrix element $\Rightarrow$ accurate benchmark for p_T of light jet radiation

Idea: look at $p_{T,j}$ spectrum in $t\bar{t}b\bar{b}$ using reduced μ_R scales and validate against NLO prediction

We consider $pp \to t\bar{t}b\bar{b}j$ at 13 TeV centre of mass energy

- top quark stable, not decayed
- jets reconstructed using anti-k_T algorithm as implemented in `FastJet-3.2`
- $\Delta R = 0.4, \quad p_T > 50$ GeV, $\quad |\eta| < 2.5$
- input parameters and scales choices as in $t\bar{t}b\bar{b}$

b-jets tagging

this talk

"single-tagged": b or $\bar{b}$ quark content

"double-tagged": $b\bar{b}$ content

generic b-jet: b, $\bar{b}$ and $b\bar{b}$ equally counted

important for comparisons against PS

Disclaimer: all results are preliminary!

OpenLoops2 for $t\bar{t}b\bar{b}j$ 1-loop MEs

The 1-loop matrix elements relevant for $t\bar{t}b\bar{b}$ and $t\bar{t}b\bar{b}j$ production are computed using

OpenLoops2: new on-the-fly helicity summation and integrand reduction [F.B., S.Pozzorini, M.Zoller '17]

→ publicly available very soon! [F.B., J.Lindert, P.Maierhöfer, S.Pozzorini, M.Zoller]

OpenLoops2 for $t\bar{t}b\bar{b}j$ 1-loop MEs

The 1-loop matrix elements relevant for $t\bar{t}b\bar{b}$ and $t\bar{t}b\bar{b}j$ production are computed using

OpenLoops2: new on-the-fly helicity summation and integrand reduction [F.B., S.Pozzorini, M.Zoller '17]

→ publicly available very soon! [F.B., J.Lindert, P.Maierhöfer, S.Pozzorini, M.Zoller]

The full hadronic prediction is provided through OpenLoops2 + SHERPA-2.2.4

← same interface as OL1

`OpenLoops2` for $t\bar{t}b\bar{b}j$ 1-loop MEs

The 1-loop matrix elements relevant for $t\bar{t}b\bar{b}$ and $t\bar{t}b\bar{b}j$ production are computed using

`OpenLoops2`: new on-the-fly helicity summation and integrand reduction [F.B., S.Pozzorini, M.Zoller '17]

→ publicly available very soon! [F.B., J.Lindert, P.Maierhöfer, S.Pozzorini, M.Zoller]

The full hadronic prediction is provided through `OpenLoops2` + `SHERPA-2.2.4` ← same interface as OL1

In the 4F scheme there are two main partonic channels (+ crossings):

$q\bar{q} \to t\bar{t}b\bar{b}g$

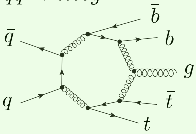

- up to rank 4 7-point 1-loop integrals
- 3534 1L Feyn. diags.
- 2^6 relevant helicity configurations

Timings[s/point] (colour + helicity sums)

	OL1	OL2+Collier	OL2+OFR
$m_b = 0$	0.337	0.208	0.233
$m_b \neq 0$	0.593	0.269	0.297

$gg \to t\bar{t}b\bar{b}g$

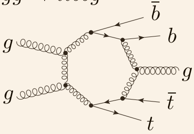

- up to rank 5 7-point 1-loop integrals
- 25431 1L Feyn. diags.
- 2^7 relevant helicity configurations

Timings[s/point]

	OL1	OL2+Collier	OL2+OFR
$m_b = 0$	4.671	1.877	2.141
$m_b \neq 0$	8.706	2.650	2.958

OpenLoops2 for $t\bar{t}b\bar{b}j$ 1-loop MEs

The 1-loop matrix elements relevant for $t\bar{t}b\bar{b}$ and $t\bar{t}b\bar{b}j$ production are computed using

OpenLoops2: new on-the-fly helicity summation and integrand reduction [F.B., S.Pozzorini, M.Zoller '17]

→ publicly available very soon! [F.B., J.Lindert, P.Maierhöfer, S.Pozzorini, M.Zoller]

The full hadronic prediction is provided through OpenLoops2 + SHERPA-2.2.4 ← same interface as OL1

In the 4F scheme there are two main partonic channels (+ crossings):

$q\bar{q} \to t\bar{t}b\bar{b}g$

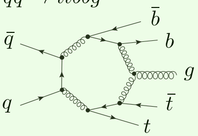

- up to rank 4 7-point 1-loop integrals
- 3534 1L Feyn. diags.
- 2^6 relevant helicity configurations

Timings[s/point] (colour + helicity sums)

	OL1	OL2+Collier	OL2+OFR
$m_b = 0$	0.337	0.208	0.233
$m_b \neq 0$	0.593	0.269	0.297

$gg \to t\bar{t}b\bar{b}g$

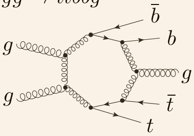

- up to rank 5 7-point 1-loop integrals
- 25431 1L Feyn. diags.
- 2^7 relevant helicity configurations

Timings[s/point]

	OL1	OL2+Collier	OL2+OFR
$m_b = 0$	4.671	1.877	2.141
$m_b \neq 0$	8.706	2.650	2.958

$+75 - 85\%$

$\sim +40\%$

OL1/OL2 up to 3!

SHERPA + OpenLoops2

$$\sigma_n^{\text{NLO}} = \int \mathrm{d}\Phi_n \left[\mathcal{B}(\Phi_n) + \mathcal{V}(\Phi_n)\right] + \int \mathrm{d}\Phi_{n+1} \mathcal{R}(\Phi_{n+1})$$

Dipole subtraction method [Catani, Seymour '96]: factorisation and universality of IR singularities

$$\mathcal{R}(\Phi_{n+1}) \to \mathcal{B} \otimes \mathcal{S}(\Phi_1) \qquad \mathcal{I} = \int \mathrm{d}\Phi_1 \mathcal{S}(\Phi_1) \Rightarrow \text{integrated analytically}$$

It allows for an IR safe numerical integration of the cross section

$$\sigma_n^{\text{NLO}} = \int \mathrm{d}\Phi_n \left[\mathcal{B}(\Phi_n) + \mathcal{V}(\Phi_n) + \mathcal{B}(\Phi_n) \otimes \mathcal{I}\right] + \int \mathrm{d}\Phi_{n+1} \left[\mathcal{R}(\Phi_{n+1}) - \mathcal{B}(\Phi_n) \otimes \mathcal{S}(\Phi_1)\right]$$

SHERPA + OpenLoops2

$$\sigma_n^{\rm NLO} = \int d\Phi_n \left[\mathcal{B}(\Phi_n) + \mathcal{V}(\Phi_n)\right] + \int d\Phi_{n+1}\mathcal{R}(\Phi_{n+1})$$

Dipole subtraction method [Catani, Seymour '96]: factorisation and universality of IR singularities

$$\mathcal{R}(\Phi_{n+1}) \to \mathcal{B} \otimes \mathcal{S}(\Phi_1) \qquad \mathcal{I} = \int d\Phi_1 \mathcal{S}(\Phi_1) \Rightarrow \text{integrated analytically}$$

It allows for an IR safe numerical integration of the cross section

$$\sigma_n^{\rm NLO} = \int d\Phi_n \left[\mathcal{B}(\Phi_n) + \mathcal{V}(\Phi_n) + \mathcal{B}(\Phi_n) \otimes \mathcal{I}\right] + \int d\Phi_{n+1} \left[\mathcal{R}(\Phi_{n+1}) - \mathcal{B}(\Phi_n) \otimes \mathcal{S}(\Phi_1)\right]$$

In `Sherpa` the dipole phase space can be restricted by means of `DIPOLE_ALPHA`

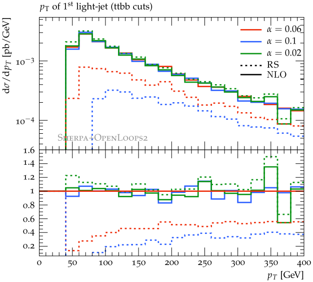

Varying α offers a check of the consistency of the subtraction

first validation of the calculation ✓

α_{dip}	NLO[pb]	BVI[pb]	RS[pb]
0.02	$3.253 \cdot 10^{-1}$	$-0.32 \cdot 10^{-1}$	$3.57 \cdot 10^{-1}$
0.06	$3.266 \cdot 10^{-1}$	$1.97 \cdot 10^{-1}$	$1.30 \cdot 10^{-1}$
0.1	$3.247 \cdot 10^{-1}$	$2.73 \cdot 10^{-1}$	$0.52 \cdot 10^{-1}$

$N_{b\text{-jets}\geq 2}$ XS

$pp \to t\bar{t}b\bar{b}j$ cross sections at 13 TeV

	$\sigma_{N_{b\text{-jets}}\geq 1}$ [pb]			$\sigma_{N_{b\text{-jets}}\geq 2}$ [pb]		
Process	LO	NLO	$\frac{\text{NLO}}{\text{LO}}$	LO	NLO	$\frac{\text{NLO}}{\text{LO}}$
$t\bar{t}b\bar{b},\ \mu_{def}$	$3.955^{+73\%}_{-39\%}$	$7.593^{+32\%}_{-27\%}$	1.92	$0.374^{+69\%}_{-38\%}$	$0.669^{+27\%}_{-25\%}$	1.79
$t\bar{t}b\bar{b},\ \mu_{gbb}$	$3.441^{+70\%}_{-38\%}$	$7.089^{+37\%}_{-28\%}$	2.06	$0.327^{+67\%}_{-37\%}$	$0.642^{+33\%}_{-27\%}$	1.96
$t\bar{t}b\bar{b}j,\ \mu_{def}$	$2.164^{+96\%}_{-45\%}$	$3.670^{+27\%}_{-30\%}$	1.70	$0.219^{+90\%}_{-44\%}$	$0.327^{+12\%}_{-25\%}$	1.49
$t\bar{t}b\bar{b}j,\ \mu_{gbb}$	$1.894^{+93\%}_{-45\%}$	$4.120^{+46\%}_{-34\%}$	2.17	$0.188^{+87\%}_{-43\%}$	$0.354^{+36\%}_{-30\%}$	1.88

- Scale uncertainty dominated by μ_R variations (as in $t\bar{t}b\bar{b}$)
- For $pp \to t\bar{t}b\bar{b}j$ $\sigma_{LO} \propto \alpha_s^5$ up to $\sim 90 - 95\%$ scale uncertainty

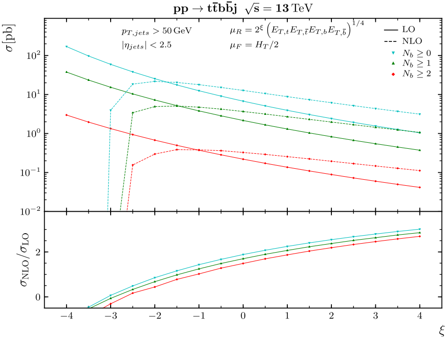

***K*-factor**:

- slightly smaller wrt $t\bar{t}b\bar{b}$ but still significant
- quite large for μ_{gbb} (1.88) bit smaller for μ_{def} (1.49)
- can be reduced by rescaling the central value

decent convergence with $\mu_{\mathbf{def}}$

b-jets distributions

We consider the phase space with two resolved b-jets

K-factor

- quite stable for both scale choices
- though more stable for μ_{gbb} over the full spectrum

Scale uncertainty at NLO

- compatible with uncertainty on the cross section:

  ranges in $\sim$ 10-25% for μ_{def}

  lives around 35% for μ_{gbb}
- for both scale choices, the uncertainty reduces in the tails
- μ_{def} shows a smaller scale uncertainty overall

  due to $\bar{\mu}_{def} < \bar{\mu}_{gbb}$

$\mu_R = \mu_{def}$ $\mu_R = \mu_{gbb}$

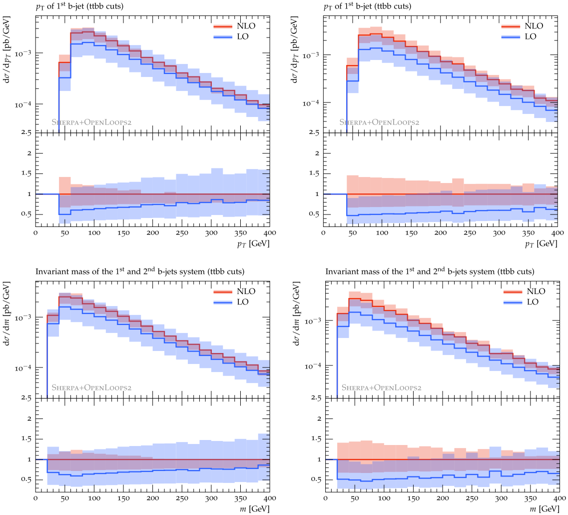

Light-jet p_T spectrum at NLO

K-factor

- shape distortions below 100-200 GeV more pronounced for μ_{def}
- more stable for μ_{gbb}

Scale uncertainty at NLO

- ranges in 20-30% up to 40-50% from bulk to the high p_T tail

$\mu_R = \mu_{def}$

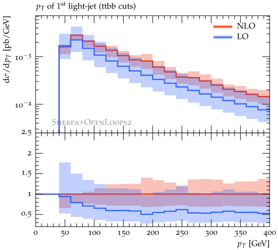

$\mu_R = \mu_{gbb}$

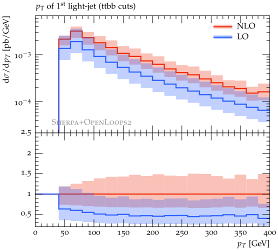

Light-jet p_T spectrum at NLO

$$\mu_R = \mu^j_{def} \qquad\qquad \mu_R = \mu^j_{gbb}$$

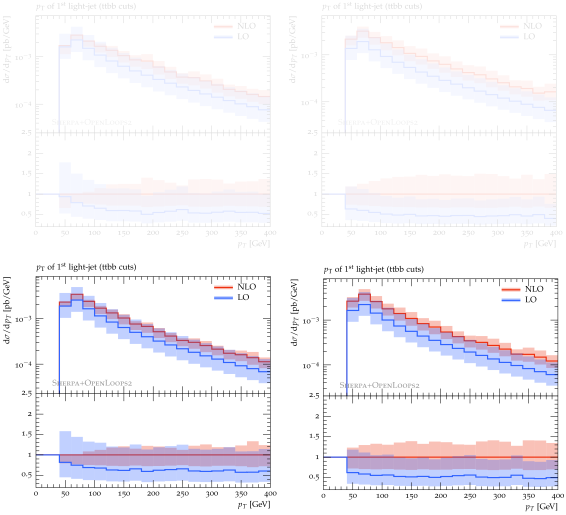

Scale choices which include jet p_T

$$\mu^j_{def} = (E_{T,t}E_{T,\bar{t}}E_{T,b}E_{T,\bar{b}}\,p_{T,j})^{1/5}$$

$$\mu^j_{gbb} = (E_{T,t}E_{T,\bar{t}}M_{T,b\bar{b}}E_{T,b\bar{b}}\,p_{T,j})^{1/5}$$

tends to reduce NLO uncertainties
and shape distortions for both scales

$t\bar{t}b\bar{b}$ vs $t\bar{t}b\bar{b}j$ NLO predictions for $p_{T,j}$

Reference scale choice: $\mu_R = \mu^j{}_{gbb} \equiv (E_{T,t}E_{T,\bar{t}}\, m_{b\bar{b}} E_{T,b\bar{b}}\, p_{T,j})^{1/5}$

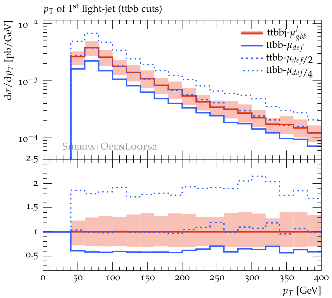

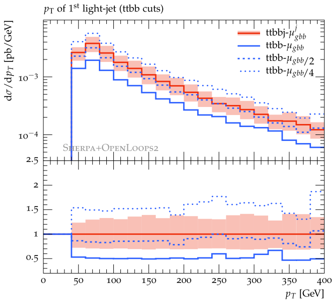

- ✓ remarkably good shape agreement over all the p_T spectrum (including region of MC disagreement)
- ✓ rescaling μ_{gbb} by 0.5 in $t\bar{t}b\bar{b}$ $\sim$ 15% agreement with NLO $t\bar{t}b\bar{b}j$
- ✓ rescaling μ_{def} by 0.5 in $t\bar{t}b\bar{b}$ $\rightarrow$ within few % agreement with NLO $t\bar{t}b\bar{b}j$

$t\bar{t}b\bar{b}$ vs $t\bar{t}b\bar{b}j$ NLO predictions for $p_{T,j}$

Reference scale choice: $\mu_R = \mu^j{}_{gbb} \equiv (E_{T,t} E_{T,\bar{t}}\, m_{b\bar{b}} E_{T,b\bar{b}}\, p_{T,j})^{1/5}$

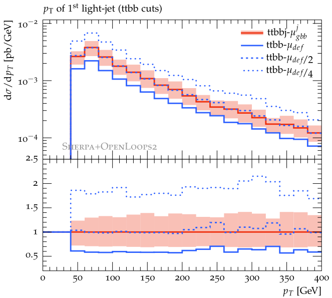

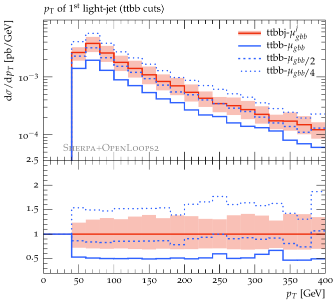

✓ remarkably good shape agreement over all the p_T spectrum (including region of MC disagreement)

✓ rescaling μ_{gbb} by 0.5 in $t\bar{t}b\bar{b}$ ∼ 15% agreement with NLO $t\bar{t}b\bar{b}j$

✓ rescaling μ_{def} by 0.5 in $t\bar{t}b\bar{b}$ → within few % agreement with NLO $t\bar{t}b\bar{b}j$

- **benchmark** with precision of ∼ 30% to **select optimal** $t\bar{t}b\bar{b}$ μ_R scale
- it motivates **reduction** of conventional $t\bar{t}b\bar{b}$ **scale** by a factor 2 (or more)
- consistent with arguments based on reduction of inclusive $t\bar{t}b\bar{b}$ K-factor

Summary

- $t\bar{t}H(H \to b\bar{b})$ searches limited by theoretical uncertainty on $t\bar{t} + b$-jets background

- crucial to understand sizeable discrepancies between NLOPS $t\bar{t}b\bar{b}$ MC on the market
  - most notably in the spectrum of extra light-jet radiation
  - related to large $t\bar{t}b\bar{b}$ NLO K-factor

- We have shown that the scale dependence of $\sigma_{t\bar{t}b\bar{b}}$ and its interplay with the m_t/m_b mass gap support a reduced μ_R choice, which would:
  - yield a smaller K-factor and a smaller scale uncertainty
  - probably mitigate NLOPS discrepancies

- We have presented NLO predictions for $pp \to t\bar{t}b\bar{b}j$
  - first application of `OpenLoops2` (with `SHERPA`)
  - provides additional support for using a reduced μ_R choice in $pp \to t\bar{t}b\bar{b}$
  - should help reducing NLOPS uncertainties (by discarding less accurate MC predictions for light-jet spectrum)

Backup slides - 1

Master formula for hardest NLOPS radation:

$$\frac{\mathrm{d}\sigma}{\Phi_\mathrm{B}} = \bar{B}_{soft}(\Phi_B)\left[\Delta(t_{IR}) + \Delta(t_1)\frac{R_{soft}(\Phi_R)}{B(\Phi_B)}\mathrm{d}\Phi_1\right] + [R(\Phi_R) - R_{soft}(\Phi_R)]\,\mathrm{d}\Phi_1$$

$$\bar{B}_{soft}(\Phi_B) = B(\Phi_B) + V(\Phi_B) + \int \mathrm{d}\Phi_1 R_{soft}(\Phi_R)$$

← NLO improved Born

POWHEG:

$$R_{soft} = R(\Phi_R)\, g_{soft}(\mu_Q, k_T)$$

MC@NLO:

$$R_{soft} = B(\Phi_B)\mathcal{K}(\Phi_1)\, g_{soft}(\mu_Q, k_T)$$

$$\mathcal{K}(\Phi_1) = \frac{\alpha}{2\pi}P(z,\phi)\frac{\mathrm{d}t}{t}\mathrm{d}z\mathrm{d}\phi$$

Jet observables

$$\frac{\mathrm{d}\sigma}{\Phi_\mathrm{B+j}} = R_{soft}(\Phi_R)\left(\frac{\bar{B}_{soft}(\Phi_B)}{B(\Phi_B)}\Delta(t_1) - 1\right) + R(\Phi_R)$$

↑ formally of $\mathcal{O}(\alpha_s)$